Earthq Eng & Eng Vib (2013) 12: 99-117 **DOI**: 10.1007/s11803-013-0155-3

Seismic demand of plan-asymmetric structures: a revisit

Rana Roy[1†] and Suvonkar Chakroborty[2‡]

1. *Department of Aerospace Engineering & Applied Mechanics, Bengal Engineering and Science University, Shibpur, India*
2. *SMS India Pvt. Ltd., SMS Group, India*

Abstract: In view of the recognition of the importance of the interdependent behavior of strength and stiffness of wall-type structural elements, the seismic demand of plan-asymmetric systems is revisited. Useful strength distribution strategies, *i.e.*, 'Center of Strength-Center of Mass (CV-CM) coinciding' and 'Balanced Center of Strength-Center of Resistance (CV-CR)' are adopted. Design charts for the seismic demand of classical uni-directionally and bi-directionally asymmetric systems are developed in a simple unified format. A conceptual framework is also outlined to conveniently apply the design charts. Illustrations are included to explain the use of the current recommendations in practical design. The study also highlights the relative performance of 'CV-CM coinciding' and 'Balanced CV-CR' criteria.

Keywords: asymmetry; seismic; strength dependent stiffness; design chart

1 Introduction

Structures are often constrained to be horizontally irregular for architectural and functional reasons. The seismic vulnerability of these systems has been observed during past earthquakes (Hart *et al*., 1975; Chandler, 1986; Rosenblueth and Meli, 1986; Esteva, 1987; Rutenberg, 1992; Goyal *et al*., 2001). Numerous investigations (e.g., Kan and Chopra, 1981a; Kan and Chopra, 1981b; Dempsey and Tso, 1982; Chopra and Goel, 1991; Tso and Zhu, 1992; Zhu and Tso, 1992; Humar and Kumar, 1998; Dutta and Das, 2002a; Dutta and Das, 2002b) have been carried out to achieve insight into the basic trend in both elastic and inelastic seismic behavior of asymmetric systems. These studies, which use a parametrically defined equivalent single story model, are well-documented elsewhere (Rutenberg, 1992; Rutenberg and Tso, 2004; Roy, 2009), and generally employ a force-based design approach.

In traditional approaches, the period of a structure is estimated and changes in its lateral strength (achieved by changing the strengths of components) are assumed to have a negligible effect on its stiffness and period (i.e., constant stiffness model). In contrast, it is well known that the yield displacement of structures responding in their predominant mode is nearly invariant for practical purpose (Priestley, 2000; Aschheim, 2002). Consequently, the stiffness of a given structure changes almost in direct proportion to the strength assigned to it (i.e., constant yield displacement model). This leads to the concept of strength-dependent stiffness as opposed to the conventional strength-independent stiffness characteristics (refer to Fig. 1). However, the majority of earlier studies and some more recent research (i.e., Dutta and Roy, 2011) explore the seismic behavior of asymmetric systems by neglecting the interdependence between strength and stiffness.

The conventional strength distribution strategy (IAEE, 2000), which emerged on the basis of existing literature, relies on the strength independent elastic stiffness of structural elements. Two useful design philosophies are conceptualized that recognize the significance of strength dependent stiffness. In the post-elastic range of shaking, during severe earthquake, the resulting resistive forces may be envisioned to pass through the center of strength (CV) of the system. If the CV is close to center of mass (CM), i.e., for a small value of strength eccentricity (e_v), only minor torque will be generated. In this circumstance, it has been shown (Paulay, 1998; Paulay, 2001a), based on plastic mechanism analyses of a number of systems, that displacement ductility demand may be minimized by minimizing the strength eccentricity, in the limit through 'CV-CM coinciding' design (i.e., $e_v = 0$). On the other hand, it is proposed and verified elsewhere (Myslimaj and Tso, 2002; Tso and Myslimaj, 2003; Myslimaj, and Tso, 2004; Myslimaj and Tso, 2005) that an efficient strength design strategy is to ensure a 'Balanced CV-CR' criterion, i.e., strength should be distributed among the load-resisting elements so that the center of strength (CV) and center of resistance (CR) is located on either side of the center of mass (CM). However, the distance

Correspondence to: Rana Roy, Department of Aerospace Engineering & Applied Mechanics, Bengal Engineering and Science University, Shibpur, India
Tel: +91-33-2668-4561; Fax: +91-33-2668-4564/2916
E-mail: rroybec@yahoo.com
†Associate Professor; ‡Deputy General Manager

Received April 3, 2012; **Accepted** November 28, 2012

of CV and CR with respect to CM depends on the performance states. Physically, such a strength design may tend to balance the elastic torque and plastic torque up to a given threshold.

The state-of-the-art review also reveals that there is latitude to explore the seismic response of a plan-asymmetric system by categorizing it into two classes depending upon the nature of prevailing stiffness eccentricity. Systems with eccentricity along one principal direction, parallel to any one side of the rigid deck, are designated as uni-directionally eccentric or mono-symmetric; whereas systems with eccentricities in two principal directions are referred to as bi-directionally eccentric. A recent study (Dutta and Roy, 2011) on low-rise multi-story systems with arbitrary variation of eccentricities in different stories also follows this classical demarcation. This classification depends on the choice of the reference axes only. In this context, the present paper examines the performance of plan-asymmetric systems, by accounting for interdependence between strength and stiffness in a unique format that precludes the customary distinction between uni-directional and bi-directional asymmetric systems. Further, the review has found that very few studies explicitly quantify the seismic demand for practical design. A recent study (Dutta and Roy, 2011) attempts to prepare a response envelope and claims the same as a design envelope. However, this study disregards the strength-dependent stiffness, and limits the demand assessment to a pair of spectrum compatible synthetic ground motions. Thus, the observations of the study may provide insight into the fundamental mechanics regulating demand amplification (such as participation of higher modes, difference in dynamic behavior between regular and irregular asymmetry, etc.) and are thus indicative of the basic trends in demand amplification. In this context, the current investigation revisits the seismic demand and accounts for strength-dependent stiffness through a comprehensive consideration of structural parameters under representative suites of ground motions. The conceptual framework is outlined and illustrated to utilize the design charts in practical design. The rationale and transparency of the proposed approach as well as the design charts furnished herein may prove useful in the design of plan-asymmetric systems.

2 Conceptual framework

This study focuses on the seismic response of plan-asymmetric systems in a unified format recognizing the strength-dependent stiffness behavior of the lateral load-resisting element. To this end, an analytical framework is established that explicitly considers the implications of strength-dependent stiffness. Companion symmetric analogues presented in Fig. 2(a) show that the lateral load-resisting elements are assumed to be oriented along two principal axes. Thus, in the related asymmetric model, eccentricities along one/both the principal axes may exist. It is customary to measure such eccentricities axis-wise (principal). Thus, in a uni-directionally eccentric system, eccentricity along one axis (e_{rx} or e_{ry}) is specified while bi-directionally eccentric systems are characterized by specifying both e_{rx} and e_{ry}. Alternatively, system asymmetry may be completely defined by specifying the distance (e_{rr}) between the center of mass (CM) and center of stiffness (CR) along the line joining CM and CR together with its angle of inclination ($e_{r\theta}$) with one of the principal axes (Fig. 2b). This simple analogy, in contrast to the traditional one, combines the general class of plan-asymmetric systems in a unique format.

In this context, it may be reiterated that the position of CR cannot be established prior to the strength assignment. However, relative yield displacement of load-resisting elements may be estimated with reasonable accuracy based only on the architectural drawings (Paulay, 2001b; Aschheim, 2002). Subsequently, the distance of reference yield displacement center (CΔ) with respect to CM (CΔ∧CM|x) may be estimated along any principal axis (i.e., x-axis) by employing the following analytical expression (refer to Appendix A for detailed derivation).

$$\mathrm{C\Delta{\wedge}CM}|_x = \left[\frac{1}{\sum_{i=1}^{n_y} \frac{\kappa_{iy}}{l_{wi_y}{}^{p}}} \left\{ \sum_{j=2}^{n_y} \frac{\kappa_{jy}}{l_{wj_y}{}^{p}} \times \left(\sum_{j=2}^{j} \eta_{(j-1)\wedge j_x} \right) \right\} \right] - \gamma_x D_x \tag{1}$$

where γ_x defines the position of the center of mass

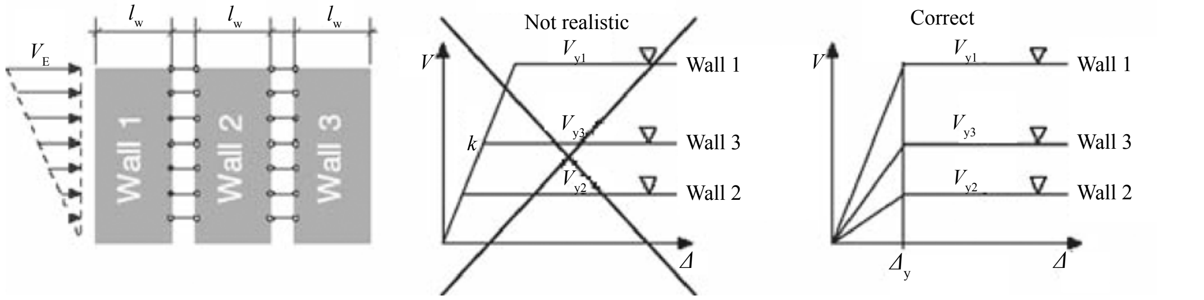

(a) Lateral load-resisting wall (b) Constant stiffness model (c) Constant yield displacement model

Fig. 1 Force-displacement relationship of wall-type elements used in Sommer and Bachmann, 2005 (extracted from De Stefano and Pintucchi, 2008)

normalized to D_x along the x-axis; l_{wi_y} is the wall length of ith element oriented along the y-axis; $\eta_{(j-1)\wedge j_x}$ is the spacing between the (j-1)th and jth element measured along the x -axis; D_x is the plan dimension of the deck along the x-direction and n_y is the number of elements oriented in the y-direction where element numbering increases in the positive direction of the axis (also refer to Fig. 2(c)). κ_{iy} is the relative strength distribution factor (ratio of element strength to strength of the system in the y-direction) and the mathematical exponent p are unity to compute C∆^CM (to be independent of strength). Similarly, $C\Delta{\wedge}CM|_y$, i.e., the distance of reference yield displacement center (C∆) with respect to CM along the y-axis, may be estimated.

It has been recognized elsewhere (Tso and Myslimaj, 2003) that the distance between the center of strength (CV) and center of resistance (CR) may be approximated to be equal to yield displacement eccentricity. Thus, C∆^CM may be indicative of the distance of CR from CM where the strength distribution is prescriptively targeted to be CV-CM coinciding; this situation is also assumed in the current investigation (Fig. 2d(i)). Subsequently, the CR may be mathematically quantified in terms of e_{rr} and $e_{r\theta}$ as

$$e_{rr} = [(C\Delta{\wedge}CM|_x)^2 + (C\Delta{\wedge}CM|_y)^2]^{0.5} \tag{2a}$$

and $$e_{r\theta} = \arctan[C\Delta{\wedge}CM|_y \div C\Delta{\wedge}CM|_x|] \tag{2b}$$

Thus, e_{rr} and $e_{r\theta}$ may be computed at the beginning of the design process with reasonable accuracy. Even when CV is not intended to match with CM (e.g., 'Balanced CV-CR' strategy as in (Fig. 2d(ii)), presuming the relative strength of the elements, the actual location of CR may be arrived at by introducing κ and setting the exponent p to -1 in Eq. (1). Since for the desired performance limit, strength distribution is often a perceptive choice of the designer, e_{rr} may be estimated with reasonable precision relative to the inherent uncertainties in seismic design.

3 Modeling of the system

A single story rigid diaphragm model with three degrees of freedom, two translations in two mutually orthogonal directions and one in-plane rotation, is used in this study. A representative dynamic model is shown in Fig. 3 for reference. A rigid diaphragm is assumed to be supported by axially inextensible load-resisting

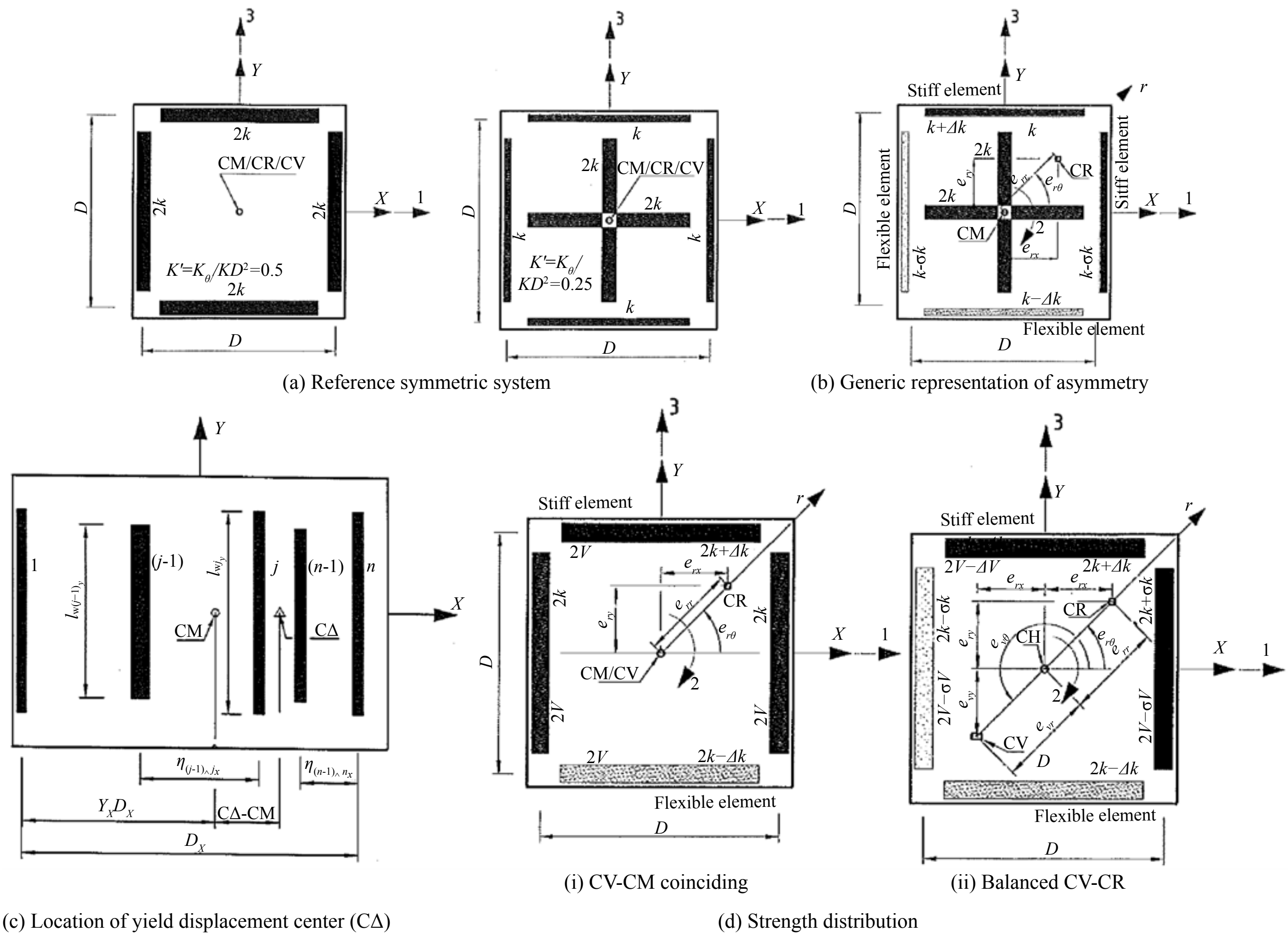

(a) Reference symmetric system

(b) Generic representation of asymmetry

(c) Location of yield displacement center (C∆)

(i) CV-CM coinciding

(ii) Balanced CV-CR

(d) Strength distribution

Fig. 2 Unified representation of equivalent single story system and associated strength distribution, *i.e.*, CV-CM coinciding and Balanced CV-CR

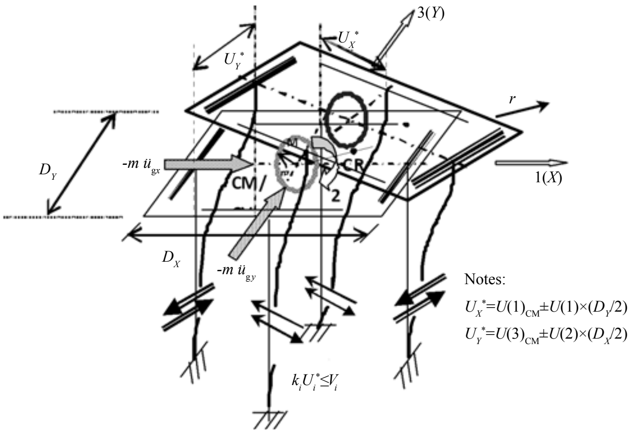

Fig. 3 Schematic diagram of reference dynamic model

elements with stiffness and strength in their planes only. Mass (M) is assumed to be distributed at the floor as regulated by the radius of gyration r_g. Under seismic excitation, standard equations of motion are used to model the system using well-known procedures (refer to Clough and Penzien, 1993). Two typical structural plan configurations with different torsional stiffness are considered (Fig. 2(a)). The implication of plan-wise distribution, explained elsewhere (Dutta, 2001), is also summarized herein. In the relevant asymmetric system, the stipulated amount of eccentricity is introduced in the parametric study by increasing the stiffness of the lateral load-resisting element of one edge by a calculated amount and decreasing it at the opposite edge by an equal amount. This does not cause any change in the overall stiffness of the idealized system. The lateral load-resisting edge element with lesser stiffness is designated as the flexible element and the opposite edge element with greater stiffness is referred to as the stiff element.

4 Ground motions

During bi-directional seismic shaking in bi-directionally eccentric structures, eccentricities along two principal directions result in two torsional moments. The effect of torsion seems to be amplified if the moments generated due to eccentricities in each direction are additive in nature, while the mutually cancelling nature of such moments tend to reduce the impact of torsion. Such addition or cancellation of two torsional moments depends on the relative sense of eccentricities regulated by the quadrant-wise location of resistance centers. For instance, in a seismic event, two systems with resistance centers in the first and second quadrant (e.g., systems located on either side of a road intersection where the street facing sides may be considered as flexible elements because of larger openings) should be subjected to different torques (two torques induced due to a pair of ground motion will be additive in one case and subtractive in the other). Further, interaction between such a pair of torsional moments (additive/cancelling) on a bi-directionally eccentric system may be additive or cancelling depending upon the ground motion characteristics (in phase or out of phase) and hence the maximum response considering both types of eccentricities are considered for design.

Seismic response may be sensitive to ground motion characteristics such as frequency content, pattern of pulses, duration of shaking, fault-rupture mechanism, etc. In this context, three suites of ground motions (short duration, SD; long duration, LD and forward directive, FD), each comprising three representative ground motion records, are used in the present study. Details of the ground motion records, selected from a related work (Aschheim and Black, 1999), are provided in Table 1. The ground motion histories and associated spectra are given in Fig. 4. Further, two uncorrelated synthetic ground motions consistent with the spectrum depicted in the Indian standard (IS 1893: 1984) are employed herein. Code-specified design spectrum and the response spectrum regenerated using this synthetic ground acceleration data (PGA = 0.1g) and presented elsewhere (Roy, 2009), are shown to have good agreement.

In this study, elastic strength demand of the reference symmetric system due to each ground motion is computed. The initial strength of the related symmetric system, recognizing apparent stability of yield displacement, may be conveniently estimated using yield displacement spectra (Aschheim, 2002). System strength computed in this way is distributed among the elements in proportion to the tributary area so that the center of strength (CV) coincides with center of mass (CM), which is a desirable strength distribution criterion particularly at the Life safety/Collapse Prevention state (Fig. 2d(i)). Limited case studies have been conducted that distribute strength so that CV and CR lie on either side of CM at an equal distance (a special case of 'Balanced CV-CR' design) as shown in Fig. 2d(ii). The response reduction factor, *R*, is considered to evaluate the seismic demand under different seismic hazards. *R* is defined as the factor by which the force demand generated if the structure were to remain elastic is reduced to obtain the design lateral force. This *R* can hence be used as a measure of the likely inelastic seismic hazard of a given structure. In the parametric study, to achieve a specific inelastic action defined by *R*, ground motion is appropriately scaled up without altering element strength. In the event of an earthquake, seismic demand depends on the degree of inelastic activity. Thus, the choice of PGA that the elastic strength is decided for is only of relative significance. Hence, although the choice of PGA value depends on the seismic activity of a particular region, the results provided herein are generic in nature.

5 Methodology

This section outlines the general framework of the

Table 1 Details of ground motions used (Aschheim and Black, 1999)

	Identifier	Date of occurrence	Magnitude	Station	Component	PGA (g)	Epicentral distance (km)
Short duration (SD)	IV79ELCN.140	Imperial valley 15 Oct 1979	$M_L = 6.5$	El Centro Array #7	140	0.338	28
	IV79ELCN.230				230	0.415	
	LP89CORR.090	Loma Prieta 17 Oct 1989	$M_W = 6.3$	Corralitos Eureka Cayon Road	90	0.463	8
	LP89CORR.000				0	0.644	
	NR94CENT.360	Northridge 17 Jan 1994	$M_W = 6.7$	Century City	360	0.222	19
	NR94CENT.090				90	0.583	
Long duration (LD)	CH85LLEO.010	Central Chile 3 Mar 1985	$M_L = 7.8$	Llolleo-Basement 1-Storey Building	10	0.712	60
	CH85LLEO.100				100	0.445	
	LN92JOSH.360	Landers 28 Jun 1992	$M_W = 7.4$	Joshua Tree	360	0.274	15
	LN92JOSH.090				90	0.284	
	TA78TABS.000	Tabas, Iran 16 Sep 1978	$M_L = 7.4$	Tabas	0	0.836	75
	TA78TABS.090				90	0.852	
Forward directive (FD)	LN92LUCN.000	Landers 28 Jun 1992	$M_W = 7.4$	Lucerne	0	0.785	42
	LN92LUCN.275				275	0.721	
	LP89SARA.000	Loma Prieta 17 Oct 1989	$M_W = 6.9$	Saratoga Aloha Avenue	0	0.512	28
	LP89SARA.090				90	0.324	
	IV79BRAW.225	Imperial valley 15 Oct 1979	$M_L = 6.5$	Brawley Airport	225	0.160	43
	IV79BRAW.315				315	0.220	

M_w: Moment magnitude, M_L: Richter magnitude and PGA: Peak ground acceleration

finite element-based computational scheme used herein for three-dimensional frame analyses in the nonlinear range. Standard system parameters such as mass, mass moment of inertia; stiffness, strength of the elements etc. are given as basic input to the program. The entire time domain is divided into a large number of time steps. In the parametric simulation, mass of the system is adjusted to achieve a target lateral uncoupled period, while different torsional periods are set to regulate the distribution of the mass by varying the radius of gyration. A simple elasto-plastic hysteresis model is used as constitutive characteristics of the load-resisting elements. For each time step, the global displacement vector at the end of the previous step is a known input (initialized as null). The displacement vector for each individual element is obtained with this input. The element displacement vector is fed as an input to the hysteresis subroutine and the elemental spring force vector is computed. These elemental spring force vectors for all elements are then assembled to obtain the global force vector. Under specified ground acceleration histories, standard equations of motion are solved in the time domain using Newmark's β-γ scheme, which considers constant average acceleration over each incremental time step. While Newmark's parameters γ and β are chosen, respectively, as 0.5 and 0.25, iterations are performed in each incremental time step using the modified Newton-Raphson technique. The time step of integration is taken as less than $T_l/1000$ second to ensure convergence (T_l is the lateral natural period of the system). Thus, the global incremental displacement vectors for the current step are calculated. 2% of critical

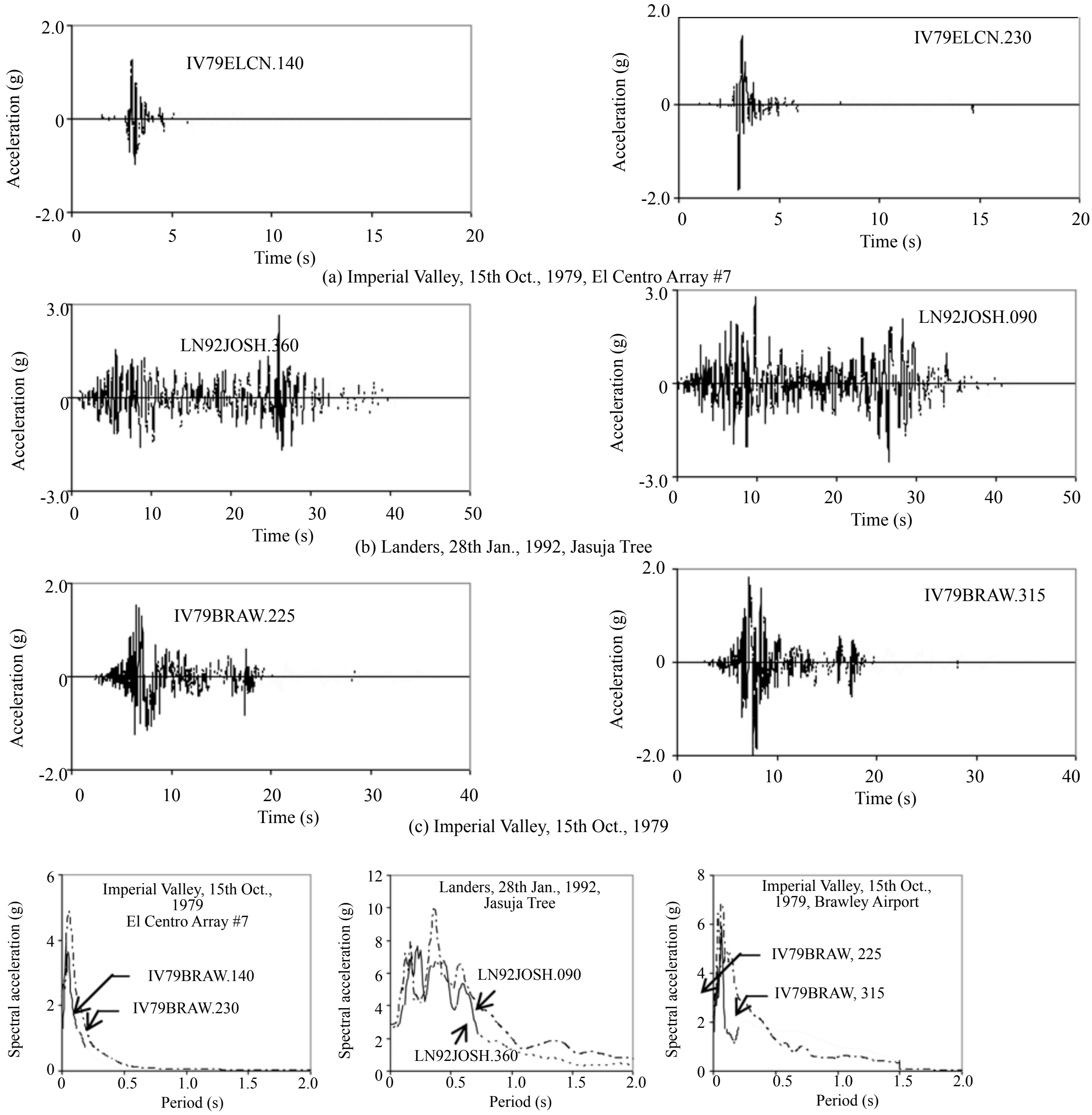

Fig. 4 Typical ground motion histories and associated spectra (a) Short duration (SD), (b) Long duration and (c) Forward directive (FD)

damping in each mode of vibration is considered to constitute the damping matrix.

6 Details of parametric studies

Systems with varying period (T_1), i.e., 0.2 s, 1.0 s and 3.0 s, representative of short, medium and long period ranges, are examined. Response reduction factor R is considered to vary as 1, 2, 4 and 6 to systematically cover the entire feasible range. The response of asymmetric structures normalized due to dynamically equivalent reference symmetric systems is presented to identify the impact of asymmetry alone. In view of the strong dependence of seismic torsional behavior on fundamental torsional-to-lateral period ratio (τ) of the corresponding uncoupled system, response quantities are estimated for different τ in the range of 0.25 to 2.0 representative of torsionally stiff and flexible systems, respectively. These parameters reflect the relative proximity of torsional and lateral period and are likely to capture the interdependent coupled behavior between lateral earthquake force and earthquake-induced torsion. Note that mass distribution is quantified through the variation of the radius of gyration (r_g), while the distribution of stiffness is expressed in terms of the parameter K_θ/K. Thus, the period ratio τ can be expressed as $r_g/(K_\theta/K)^{0.5}$. However, it is obvious that several combinations of r_g and K_θ/K are possible corresponding to a unique value of $r_g/(K_\theta/K)^{0.5}$. This implies that more than one structure with identical τ and T_1 may exist corresponding to different combinations of mass and stiffness distribution. In order to distinguish these structures, the K_θ/K ratio is therefore specified. In this context, the current investigation primarily considers normalized stiffness parameter $K_\theta/(KD^2)$ as 0.5, while a few cases with $K_\theta/(KD^2)$ equals to 0.25 are analyzed for comparison. In numerical simulation, uncoupled lateral periods of these systems are set by suitable adjustment of mass; meanwhile, the mass moment of inertia is varied by specifying r_g to achieve different torsional periods.

7 Results and discussions

The response of systems with different eccentricities is computed under bi-directional ground motion applied along two principal directions of the system. Maximum in-plane deformation of the edge elements (U^* as in Fig. 3) due to the coupled effect of translation and torsion over the entire earthquake history is normalized by those of the reference symmetric model. The quantities computed for load-resisting elements orientated in both the principal directions are compared for flexible and stiff sides separately and the greatest ones are referred to herein as maximum normalized element displacement

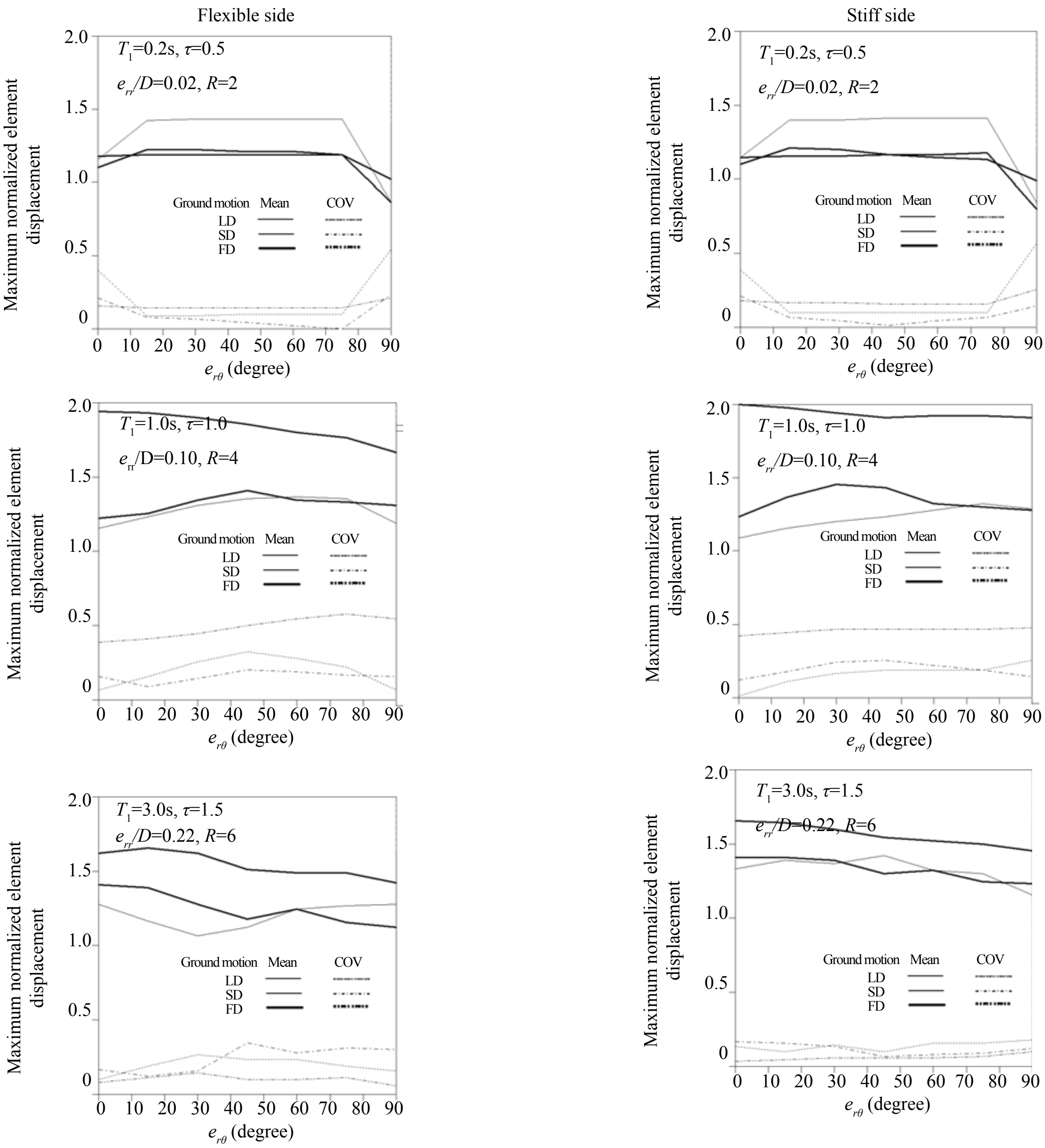

Fig. 5 Variation of maximum normalized displacement response with change of $e_{r\theta}$

of the respective side. Figure 5 describes the variation of the maximum normalized element displacement for both flexible and stiff sides as a function of $e_{r\theta}$, while a similar variation with change of e_{rr}/D is presented in Fig. 6. These curves describe the variation of the mean of responses under a set of ground motions belonging to a predefined category, i.e., LD, SD and FD. The results also include the coefficient of variation (COV) of the relevant response parameter with reference to the categories of ground motion records used. Combinations of other influential parameters are chosen to cover torsionally flexible to stiff systems with various lateral periods and different degrees of inelastic excitation defined by R. On the basis of the exhaustive case studies, it is shown that the impact of asymmetry, for short period system, seems to be paramount under LD ground motion (Mean: 1.4 to 1.70 and COV: 0.25), while the same generally attains the peak under the FD type of record for medium (Mean: 1.5 to 2.0 and COV: 0.25) and long period (Mean: 1.7 to 3.0, COV: 0.25 to 0.32) systems.

It is perceived that the accumulated plastic strain in load-resisting structural elements during several cycles of repetitive loading may be a more rational parameter to assess damage. To this end, the influence of lateral-torsional coupling on the inelastic range response is also assessed through normalized hysteretic energy ductility demand (NHEDD denoted as μ_H) (Mahin and Bertero 1981). Physically, this implies the ratio between the equivalent displacements required by a similar elasto-plastic system to dissipate an equal

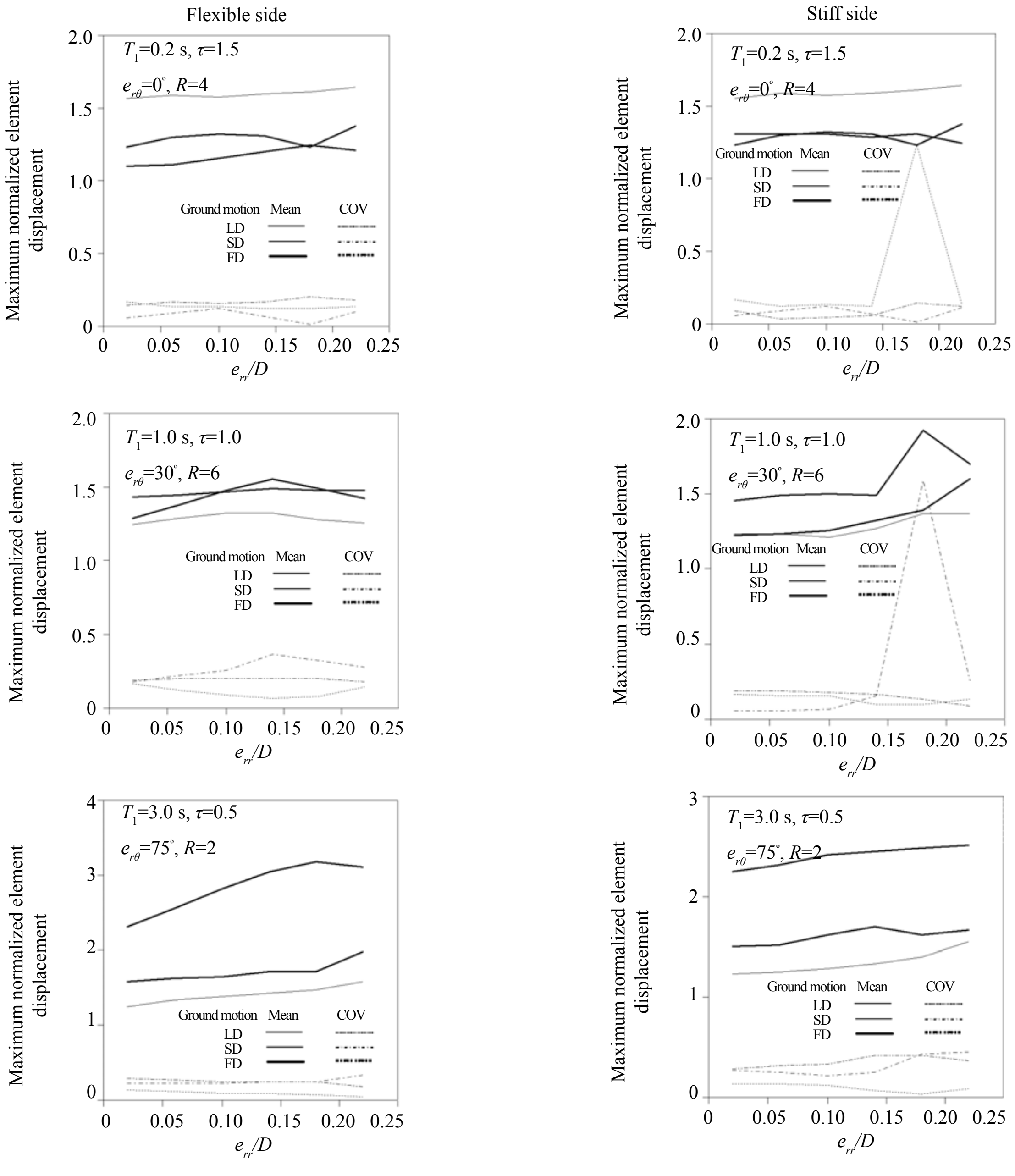

Fig. 6 Variation of maximum normalized displacement response with change of e_{rr}/D

amount of energy as that in the original system under a monotonic loading and the yield displacement. The variation of the maximum normalized hysteretic energy ductility demand, normalized by the same quantity from an associated symmetric system (μ_{H0}), i.e., μ_H/μ_{Ho}, is presented in Fig. 7 and Fig. 8. Variation in response, to a lesser extent, appears to be sensitive to the parameter $e_{r\theta}$ and generally reflects an increasing trend as e_{rr}/D is increased for stiff sides. A comparison of Fig. 5 and Fig. 6 with Fig. 7 and Fig. 8 shows a greater sensitivity of the accumulated damage index (μ_H/μ_{Ho}) relative to the maximum normalized element displacement with the change of the system eccentricity, i.e., $e_{r\theta}$ and e_{rr}/D.

Recognizing the sensitivity of seismic response of asymmetric systems to the plan-wise distribution of load-resisting elements, response for similar systems with $K_\theta/(KD^2)$ equals to 0.5 and 0.25 over a wide range of variation of τ (0.25–2.0) is examined under synthetic ground motions and furnished in Fig. 9. Response arising out of such plan-wise distribution, though not consistent, seems to be influenced particularly at low response reduction factor and tends to be less sensitive for higher response reduction factor (R).

In this perspective, it may be interesting to examine the efficacy of the 'Balanced CV-CR' design technique using the 'CV-CM coinciding' design strategy. In this type of parametric study, strength and stiffness centers are spaced at a distance of 0.025 D on either side of the CM in the 'Balanced CV-CR' design, resulting in e_{rr} = 0.025 D and $e_{r\theta} = 90^0$. However, the equal distance of CV

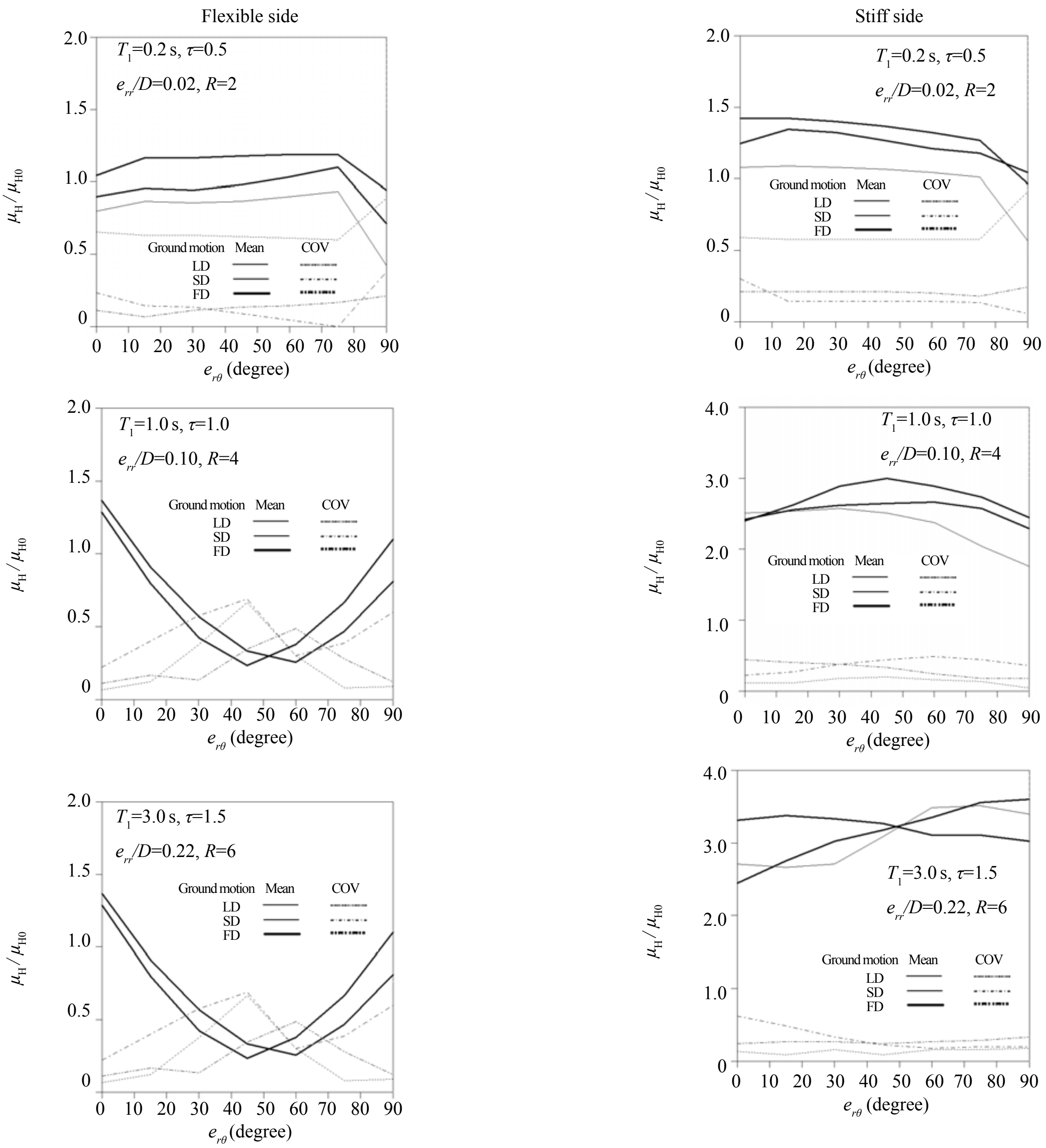

Fig. 7 Variation of maximum normalized hysteretic energy ductility demand with change of $e_{r\theta}$

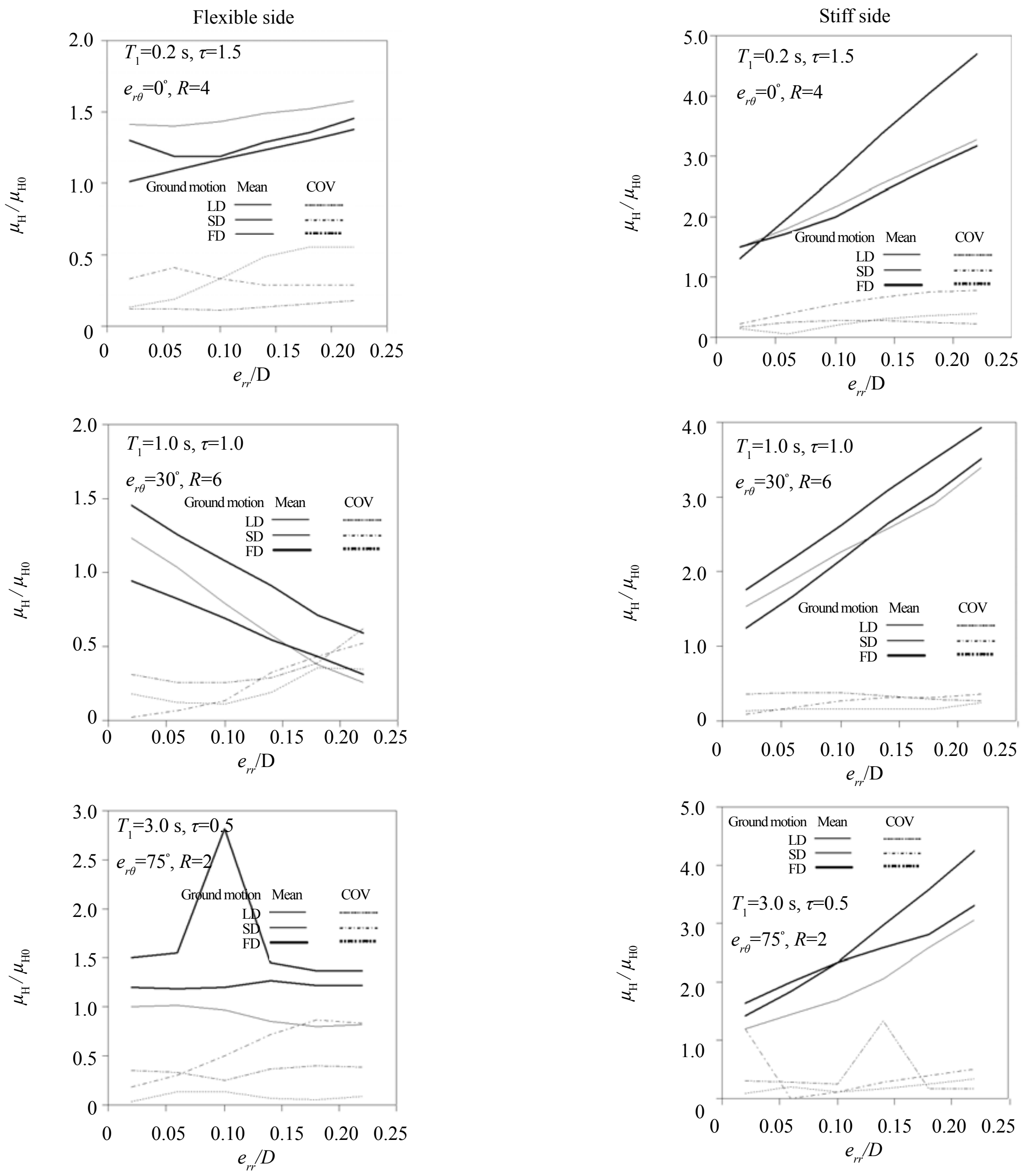

Fig. 8 Variation of maximum normalized hysteretic energy ductility demand with change of e_{rr}/D

and CR with respect to CM as chosen herein is a typical one and actually depends on the performance state. On the other hand, e_{rr} = 0.5D and $e_{r\theta}$ = 90° is assumed in the 'CV-CM coinciding' design approach. These systems are analyzed under code-compatible synthetic ground motion for a wide range of τ and representative R. The results are presented in Fig. 10 and reveal a better performance of the 'CV-CM coinciding' design strategy relative to the 'Balanced CV-CR' for higher R factors, which indicates higher seismic hazards. However, the performance of the 'Balanced CV-CR' design appears to be comparable under minor earthquakes. In the framework of performance based design, this implies that for design performance states such as Life safety or Collapse prevention, The 'CV-CM coinciding' design may be preferred; while the performance of the 'Balanced CV-CR' design appears to be comparable at the Immediate Occupancy Level (Vision 2000, 1995). This observation is physically intuitive. In the Life Safety and Collapse Prevention Level, the load-resisting elements have a propensity to be more in the plastic domain during the seismic event and hence minimizing strength eccentricity leads to a better performance under these circumstances,.

It may be envisioned that the performance of both the proposed strength design techniques seems sensitive to the pre-yield and post-yield duration of load-resisting elements and hence on ground motion characteristics.

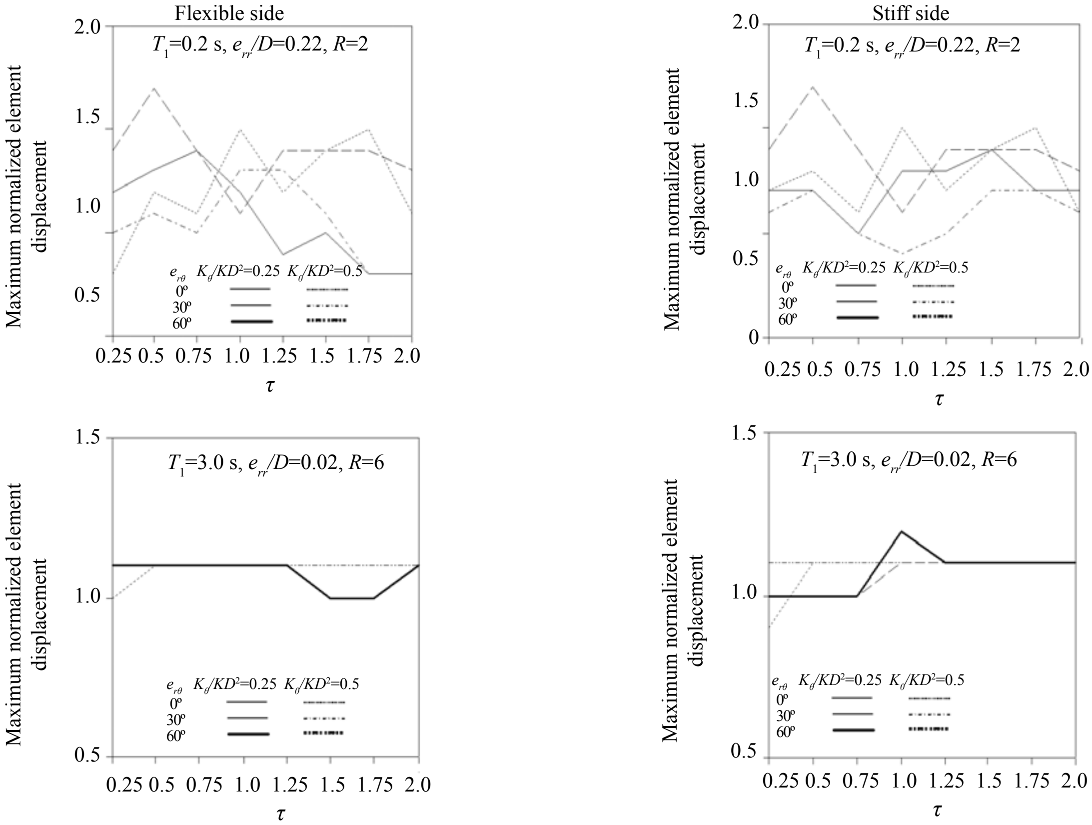

Fig. 9 Comparison of response of systems with different plan-wise distribution

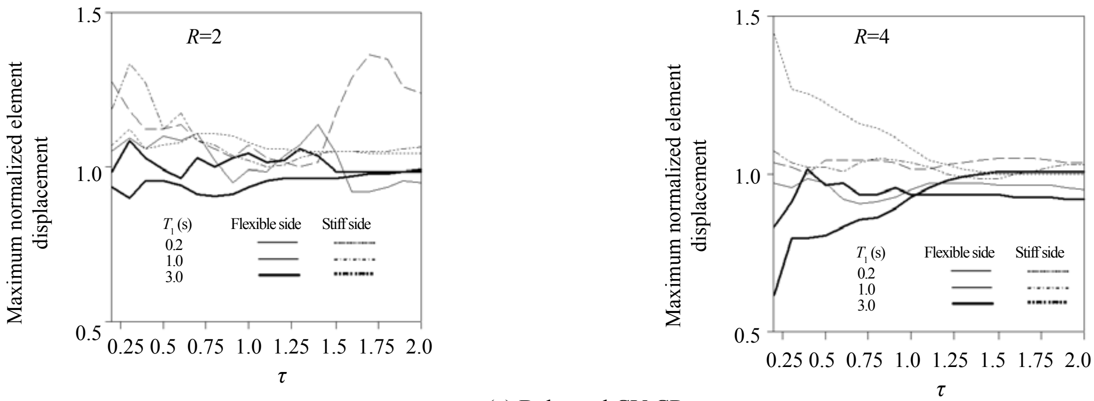

(a) Balanced CV-CR

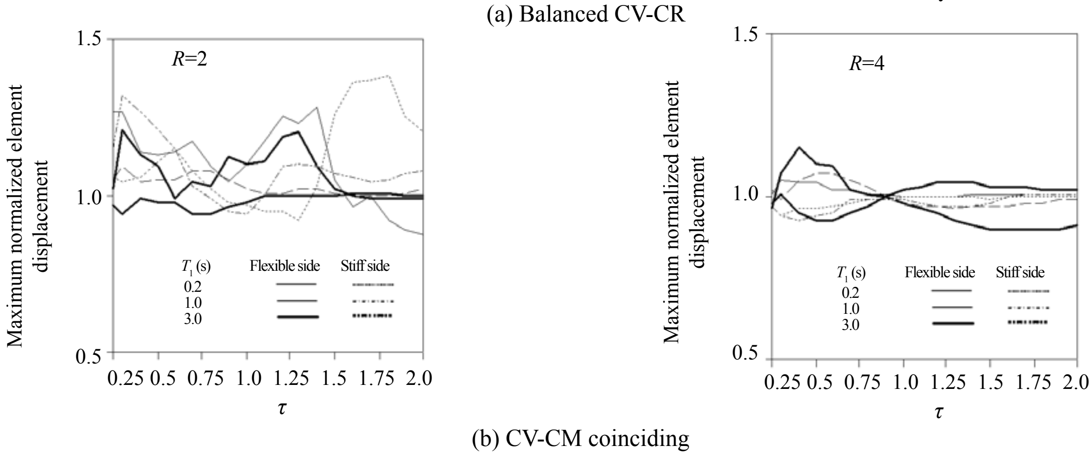

(b) CV-CM coinciding

Fig. 10 Performance of 'Balanced CV-CR' and 'CV-CM coinciding' strength distribution

The relative performance of these two design strategies, therefore, deserves further investigation using ensembles of ground motion records.

8 Design recommendations

Upon closer scrutiny of the variation in response (Fig. 5 to Fig. 10), it is recognized that a definitive trend in the inelastic seismic response does not appear possible. Rather, a compilation of the comprehensive case studies covering different system parameters and representative ground motions reveals potential dispersion in the computed results (COV ranges between 0.01 to 1.51). In this context, the response of systems with different dynamic characteristics (i.e., T_1 and τ) and degree of asymmetry (quantified by e_{rr} and $e_{r\theta}$) is computed for various R under the three sets of ground motions (SD, LD and FD) considered herein. these response quantity is normalized by that due to the corresponding symmetric counterpart to evaluate the amplification in response for both flexible and stiff sides. Observing the trendless variation in response and also in view of uncertainties of the characteristics of future earthquakes, for the purpose of design, normalized response quantities are averaged without regard to the distinction among SD, LD and FD characteristics of ground motion data. Thus, the mean of such normalized amplification factors are presented in Fig. 11 to Fig. 13 in the form of concentric semi-circles. Radial distances physically represent normalized e_{rr}, while the $e_{r\theta}$ value is provided on the radial lines. The amplification factor is presented at the intersection between the radial and semi-circular lines. Design charts for short, medium and long period systems corresponding to τ = 0.5, 1.0 and 1.5 are given in Fig. 11 and Fig. 12 under different performance states (R = 2, 4). The quantities for τ = 0.5 and 1.5 are also presented in Fig. 13 under severe seismic hazards (R = 6). It may be observed that these magnification factors for $e_{r\theta}$ equals to 0° and 90°, both representing so-called mono-symmetric systems, are different due to the difference in characteristics of ground motion components and the maximum should be taken for design. The mean amplification factor read from the design curves may be modified, at the discretion of the designer, by adding $I\sigma$ where I is the importance factor and σ is the standard deviation. To this end, the importance factor recommended in seismic design codes may be used and standard deviation may be computed using COV as 0.25. These curves are believed to be useful to readily assess the seismic demand of a system if the values of T_1, τ and design R are known. The seismic demand can be estimated from the uncoupled lateral and torsional periods of the structure using the simple procedure outlined in Appendix A and defined in a recent study (Dutta and Roy, 2011). The parameters that define system asymmetry (i.e., e_{rr} and $e_{r\theta}$) may be estimated using formulations outlined in Eqs. (1) and (2). It may, however, be noted that after evaluation of the seismic demand from the design chart, it is necessary to trace back the flexible and stiff sides of the systems by simple physical inspection. This may also be arrived at by locating CΔ following Eq. (1) as CR should be located at an equal distance (CΔ^CM) apart from CM on the extension of the line joining CM and CΔ to the diagonally opposite quadrant. For example, if CΔ is located in the first quadrant, CR should be in the third quadrant and vice-versa. The actual location of CR may also be obtained, in general, by equation (1) substituting suitable values of κ (using p = -1).

A single-story building consisting of a square concrete deck of dimension D_x (= D_y =10 m) and weight W of 900 kN is used to further explain the use of the design charts. The building is supported by reinforced concrete flexural walls oriented in the x-direction and y-direction, respectively (see Fig. 14). All the walls have a height of 7.5 m and thickness of 0.3 m. The length of the x-direction walls are 2.5 m and 3.0 m (E_3 and E_4), respectively. The length of the y-direction walls are 2.0 m and 3.5 m (E_1 and E_2), respectively. The nominal design strength in both directions is 0.19 W, i.e., 171 kN (say for R = 4). The yield strength of the reinforcing bar is 300 MPa and the Young's modulus of concrete is 2×10^5 MPa. The amplification of the seismic demand is estimated step-by-step and is provided in Table 2(a) and Table 2(b). For the present problem, mean amplification is estimated to be 1.56 and 1.55 for the flexible and stiff sides, respectively. Thus, in design, magnification in demand, assuming an importance factor I of the structure as unity, may be taken as 1.95 and 1.94 for flexible and stiff sides (taking COV = 0.25).

9 Summary and conclusions

In the perspective of performance-based design (Priestley, 2000) and recognition of strength dependent stiffness attributes of structural elements, existing codified provisions for the design of plan asymmetric systems does not appear conceptually sound. In this context, the present study attempts to comprehensively assess the amplification in response induced due to torsion in a rational framework. Observations presented in the form of design charts are useful without regard to the uni-directional or bi-directional nature of eccentricity of the system. The study may be summarized into the following broad conclusions:

(1) In light of the interdependence between strength and stiffness, in many design contexts, the location of CR may be estimated with reasonable accuracy employing the formulation developed herein in systems where CV coincides with CM; which is often a desirable strategy in Life Safety and Collapse Prevention design levels. A thoughtful application of the same technique is perceived to yield adequate results for systems designed with the 'Balanced CV-CR' technique.

(2) The study proposes a generic yet simple format to evaluate the seismic response of plan-asymmetric

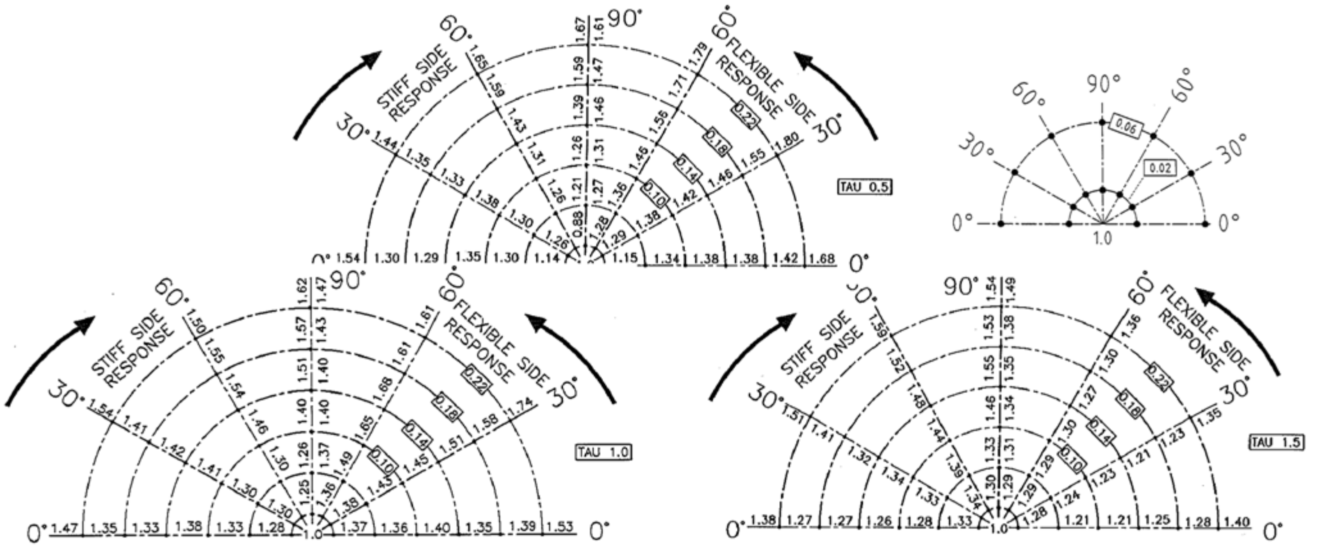

(a) Short period system

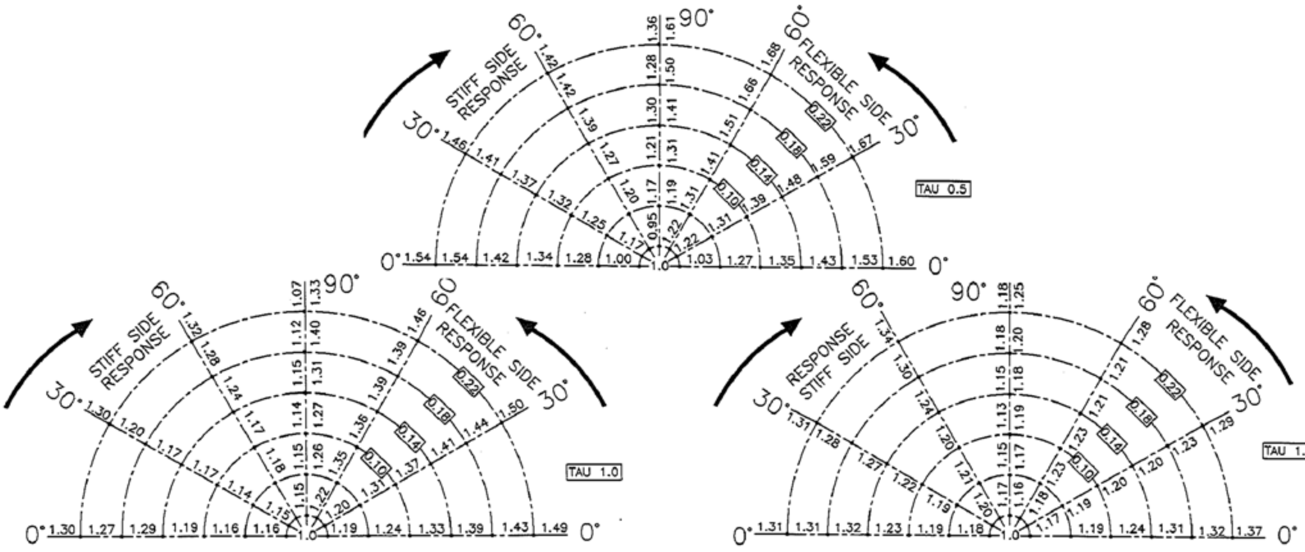

(b) Medium period system

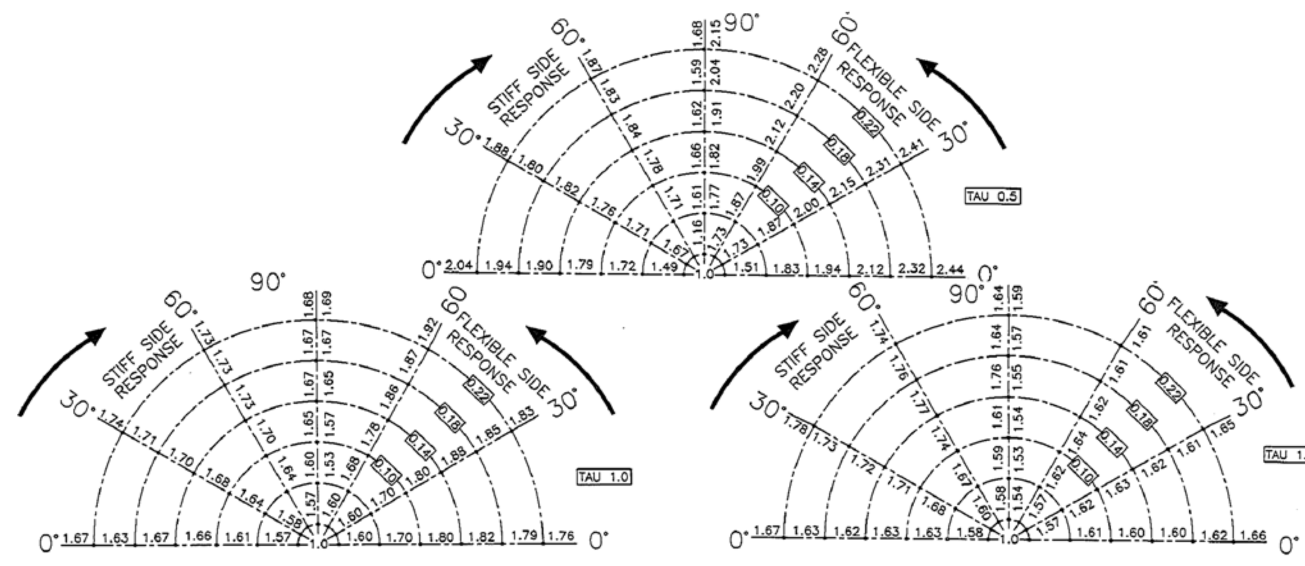

(c) Long period system

Fig. 11 Design chart for systems with varying torsional resistance under minor seismic hazard (*R* = 2)

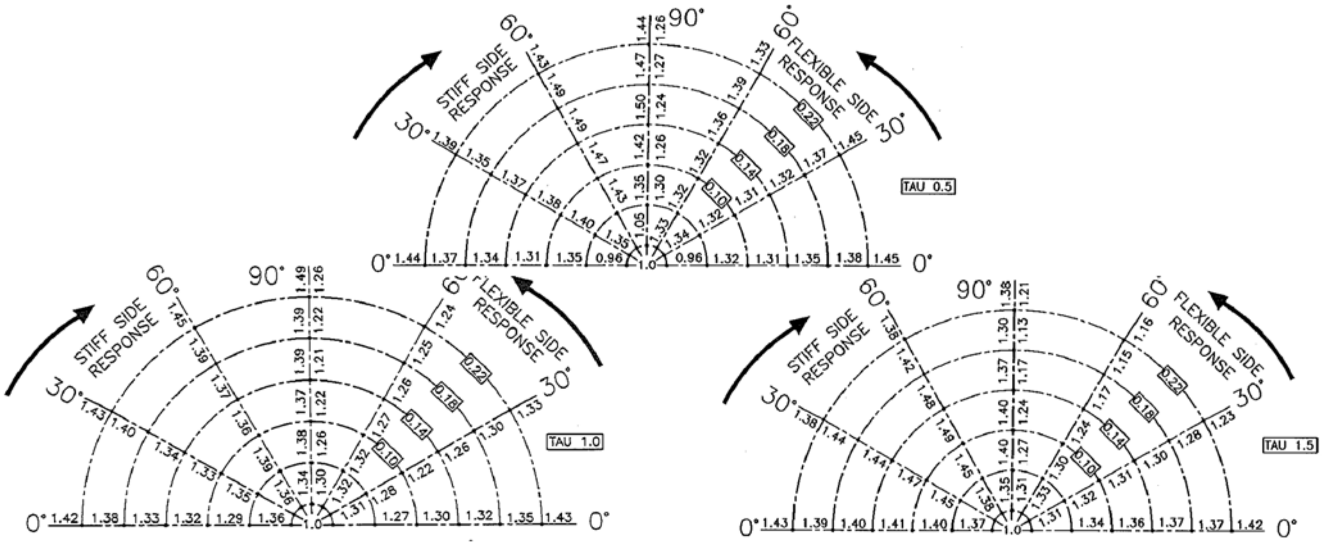

(a) Short period system

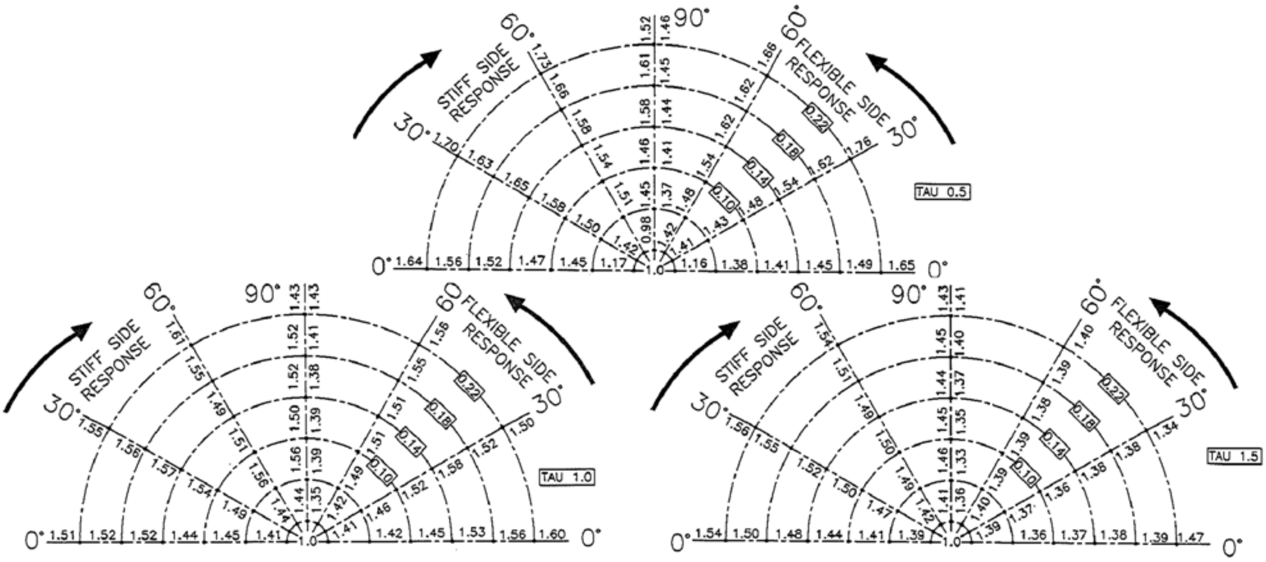

(b) Medium period system

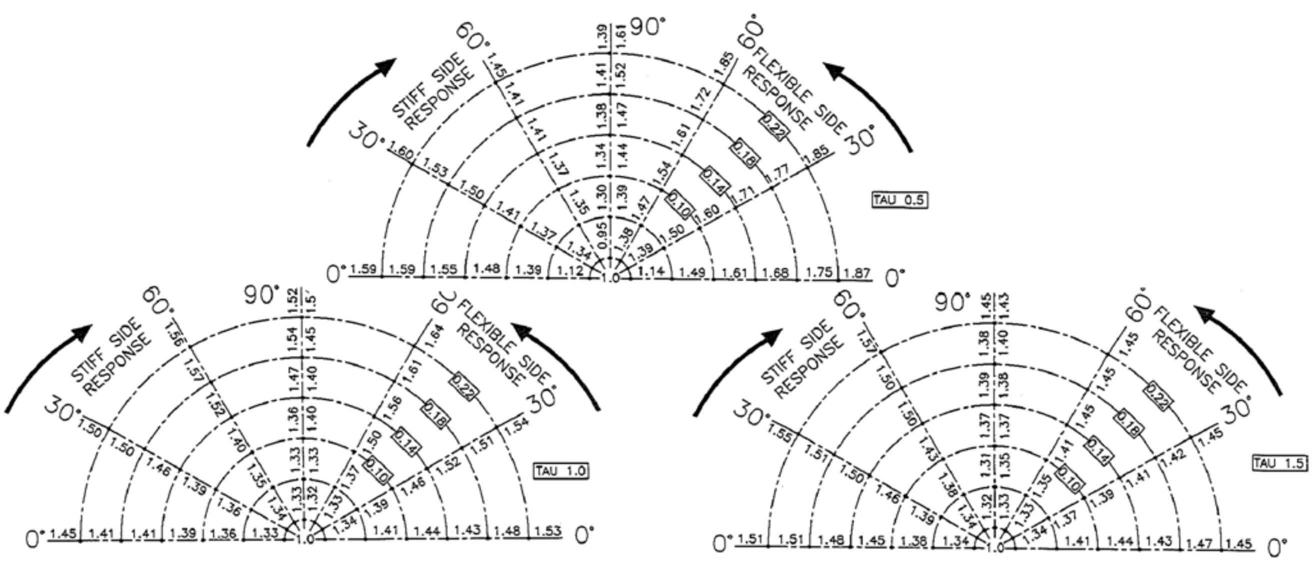

(c) Long period system

Fig. 12 Design chart for systems with varying torsional resistance under moderate seismic hazard (R = 4)

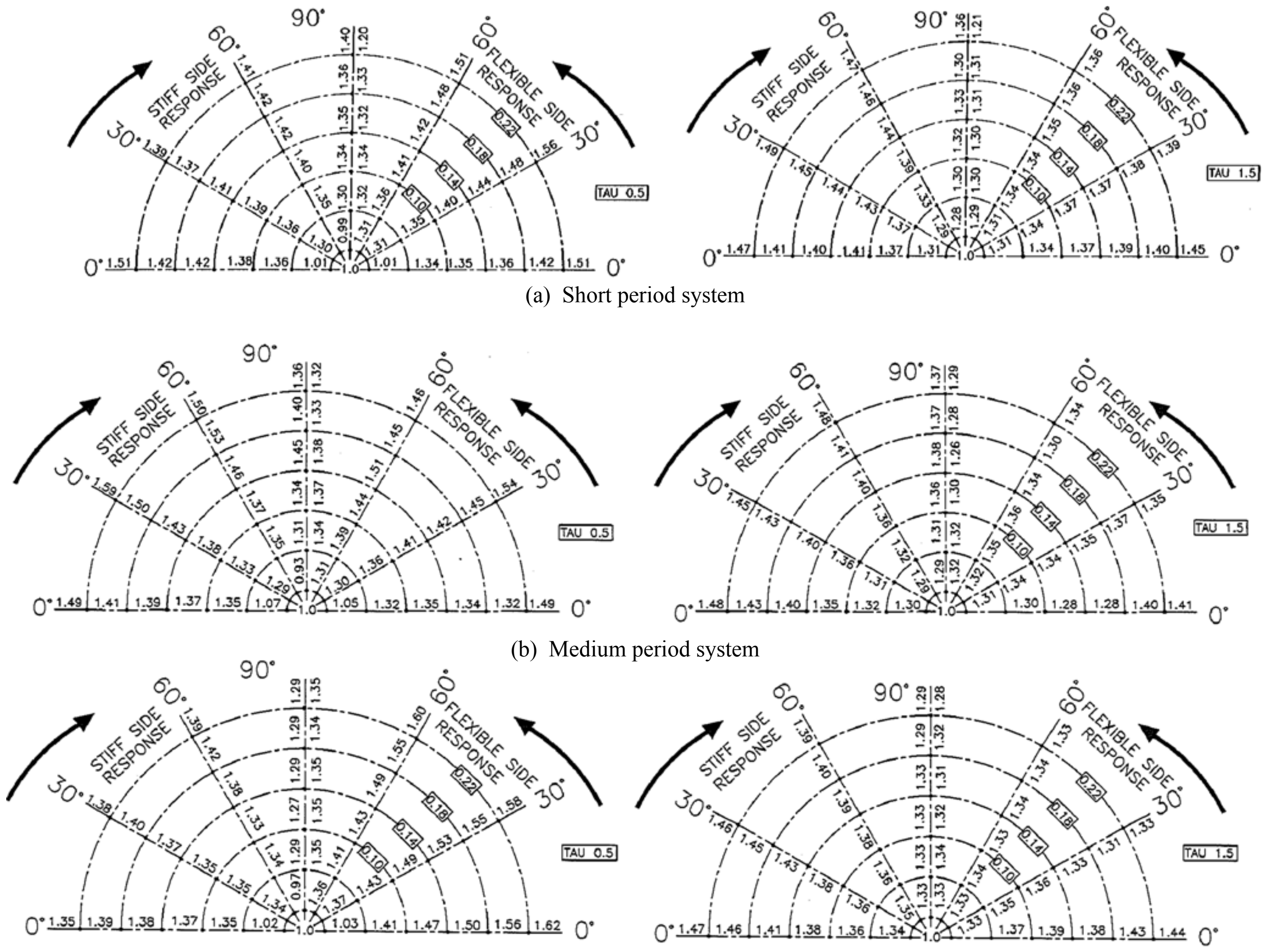

(a) Short period system

(b) Medium period system

(c) Long period system

Fig. 13 Design chart for systems with varying torsional resistance under severe seismic hazard (R = 6)

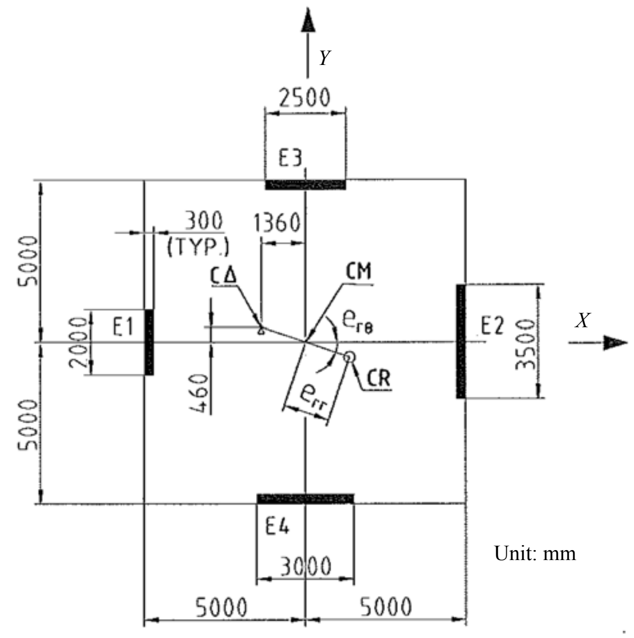

Fig. 14 Layout of example building frame with asymmetry

systems in lieu of the conventional approach that distinguishes systems as uni-directionally and bi-directionally asymmetric. It is advocated that the choice of one reference axis aligned along a line joining the CM and CR of the system and the other normal to it, always leads to a unique representation of all categories of the plan-asymmetric system.

(3) Seismic vulnerability of plan-asymmetric structures appears to be sensitive to the characteristics of ground motions. The effect of asymmetry for short period systems seems to be paramount under LD ground motion; while these systems generally attain their peak under FD type records for medium and long period systems.

(4) Seismic response, albeit sensitive to the plan-wise distribution of lateral load-resisting elements, appears to bear marginal relevance for greater R, i.e., in Life Safety and Collapse Prevention levels.

(5) The 'CM-CV coinciding' strength design strategy tends to offer superior performance, particularly in the Life Safety and Collapse Prevention levels. However, the performance of this strength design seems

Table 2a Characteristics of the example system

Element No.	Yield displacement	Nominal yield strength	Lateral stiffness: Element	Lateral stiffness: System		Torsional stiffness	Lateral period		Torsional period
	Δ_{yi} (mm)	V_{ni} (kN)	K_i (kN/m)	K_X (kN/m)	K_Y (kN/m)	K_θ (kNm)	T_X (s)	T_Y (s)	T_θ (s)
E1	28.10	86.25	3069		8426	421802		0.65	0.59
E2	16.10	86.25	5357						
E3	22.50	86.25	3833	8445			0.65		
E4	18.70	86.25	4612						

Table 2b Measurement of asymmetry and amplification in response

Element No.	l_{wi}		$\eta_{(j-1)\wedge j}$		$\mathrm{C\Delta{\wedge}CM}$*1		e_{rr}	$e_{r\theta}$	Response from design chart at $e_{rr}/D = 0.14$ [Fig. 11(b)]				Response by interpolation		Remark
	X	Y	X	Y	X	Y			$e_{r\theta} = 0.0$		$e_{r\theta} = 30.0$		$e_{r\theta} = 18.7$		
	(m)		(m)		(m)		(m)	(degree)	Flex.	Stiff	Flex.	Stiff	Flex.	Stiff	
E1		2.0		10	-1.36		1.44	18.7	1.53	1.52	1.58	1.57	1.56	1.55	CR in quadrant IV as CΔ in II
E2		3.5													
E3	2.5		10			0.46									
E4	3.0														

Note: *1 $\kappa = 1.0$ and $p = 1$; $\gamma_x = \gamma_y = 0.5$, $D_x = D_y = 10$ m, $n_y = n_x = 2$; $\tau = 0.91 \approx 1.0$

Check: Substituting $\kappa = 0.5$ and $p = -1$ in equation (1), $\mathrm{C\Delta{\wedge}CR}|_x = 1.36$ and $\mathrm{C\Delta{\wedge}CR}|_y = -0.46$

comparable to the particular case of 'Balanced CV-CR design' adopted herein for the Immediate Occupancy level.

(6) Combining the preceding two conclusions, it is shown that in regions of severe seismic activity, the observations presented herein tend to be generic irrespective of the plan-wise distribution of the load-resisting elements.

(7) The design charts presented herein for various edge elements cover a wide range of variation in the dynamic characteristics of systems and performance states may be judiciously used as convenient design-aids. For important structures and zone-specific characteristics of ground motion, these guidelines may offer preliminary information relevant to the seismic vulnerability of the system. To this end, the torsional-to lateral period ratio of the system may be conveniently evaluated using the formulation outlined in Appendix A.

To summarize, this study evaluates the seismic behavior of plan-asymmetric systems while recognizing the strength-dependent stiffness behavior of lateral load-resisting elements. Design charts are prepared in a unique format and developed through comprehensive case studies that cover representative system parameters. Observing the variation in response, in the opinion of the authors, the 'CV-CM coinciding' strength design strategy may be employed for structures located in regions of moderate to high seismic activity. The observations made herein are also believed to be applicable to torsionally coupled multistory systems with regular asymmetry. Fundamental uncoupled lateral and torsional periods of these systems, assuming uniform distribution of mass and stiffness over stories, may be estimated by multiplying the relevant expressions in Eqs. (A 2.1) and (A 2.2) by a factor equal to $\left[\frac{N\times(N+1)}{2}\right]^{0.5}$, where N represents the number of stories (Dutta and Roy, 2011).

References

Aschheim M (2002), "Seismic Design Based on the Yield Displacement", *Earthquake Spectra*, **18**(4): 581–600.

Aschheim M and Black E (1999), "Effects of Prior Earthquake Damage on Response of Simple Stiffness-degrading Structures," *Earthquake Spectra*, **15**(1): 1–24.

Chandler AM (1986), "Building Damage in Mexico City

Earthquake," *Nature*, **320**: 497–501.

Chopra AK and Goel RK (1991), "Evaluation of Torsional Provisions in Seismic Codes," *Journal of Structural Engineering*, ASCE, **117**(12): 3762–3782.

Clough RW and Penzien J (1993), *Dynamics of Structures*, McGraw-Hill Inc., International Edition.

Dempsey KM and Tso WK (1982), "An Alternative Path to Seismic Torsional Provisions," *Soil Dynamics and earthquake Engineering*, **1**(1): 3–10.

De Stefano, M and Pintucchi, B (2008), "A Review of Research on Seismic Behavior of Irregular Building Structures Since 2002," *Bulletin of Earthquake Engineering*, **6**(2): 285–308.

Dutta SC (2001), "Effect of Strength Deterioration on Inelastic Seismic Torsional Behavior of Asymmetric R/C Buildings," *Building and Environment*, **36**(10): 1109–1118.

Dutta SC and Das PK (2002a), "Inelastic Seismic Response of Code-designed Reinforced Concrete Asymmetric Buildings with Strength Degradation," *Engineering Structures*, **24**(10): 1295–1314.

Dutta SC and Das PK (2002b), "Validity and Applicability of Two Simple Models to Assess Progressive Seismic Damage in R/C Asymmetric Buildings," *Journal of Sound and Vibration*, **257**(4): 753–777.

Dutta SC and Roy R (2011), "Seismic Demand of Low-rise Multistory Systems with General Asymmetry," *Journal of Engineering Mechanics Division*, ASCE, **138**(1): 1–11.

Esteva L (1987), "Earthquake Engineering Research and Practice in Mexico after the 1985 Earthquakes," *Bulletin of the New Zealand National Society for Earthquake Engineering*, **20**(3): 159–200.

Goyal A, Sinha R, Chaudhari M and Jaiswal K (2001), *Damage to R/C Structures in Urban Areas of Ahmedabad and Bhuj, EERI Preliminary Reconnaissance Report on Earthquake in Gujrat, India*, Earthquake Engineering Research Institute, Oakland, California, U.S.A.

Hart GC, DiJulio RM and Jr. Lew M (1975), "Torsional Response of High-rise Buildings," *Journal of Structural Engineering*, ASCE, **101**(ST2): 397–415.

Humar J L and Kumar P (1998), "Torsional Motion of Buildings during Earthquakes. I. Elastic Response," *Canadian Journal of Civil Engineering*, **25(**5): 898–916.

International Association for Earthquake Engineering (IAEE), 2000, *Regulation for Seismic Design-A World List*, Tokyo.

IS 1893 (Part 1): 1984. *Indian Standard Criteria for Earthquake Resistant Design of Structures*, Bureau of Indian Standards, New Delhi, India.

Kan CL and Chopra AK (1981a), "Simple Model for Earthquake Response Studies of Torsionally Coupled Buildings," *Journal of Engineering Mechanics Division,* ASCE, **107**(EM5): 935–951.

Kan CL and Chopra AK (1981b), "Torsional Coupling and Earthquake Response of Simple Elastic and Inelastic Systems," *Journal of Structural Division,* ASCE, **107**(ST8): 1569–1587.

Mahin SA and Bertero VV (1981), "An Evaluation of Inelastic Seismic Design Spectra," *Journal of Structural Engineering*, ASCE, **107**(9): 1777–1795.

Myslimaj B and Tso WK (2002), "A Strength Distribution Criterion for Minimizing Torsional Response of Asymmetric Wall-type Systems," *Earthquake Engineering and Structural Dynamics*, **31**(1): 99–120.

Myslimaj B and Tso WK (2004), "Desirable Strength Distribution for Asymmetric Structures with Strength-stiffness Dependent Elements," *J. Earthquake Eng*., **8** (2): 231–248.

Myslimaj B and Tso WK (2005), "A Design-orineted Approach to Strength Distribution on Single-story Asymmetric Systems with Elements Having Strength-Dependent Stiffness," *Earthquake Spectra*, **21**(1): 197–212.

Paulay T (1998), "A Mechanism-based Design Strategy for Torsional Seismic Response of Ductile Buildings," *European Earthquake Engineering*, **2**: 33–48.

Paulay T (2001a), "Some Design Principles Relevant to Torsional Phenomena in Ductile Buildings," *Journal of Earthquake Eng*. **5**(3): 273–308.

Paulay T (2001b), "A Re-definition of the Stiffness of Reinforced Concrete Elements and Its Implications in Seismic Design," *Structural Engineering International*, **11**(1): 36–41.

Priestley MJN (2000), "Performance Based Seismic Design," *Proc. of 12th World Conference on Earthquake Engineering*, Auckland, Paper No. 2831.

Rosenblueth E and Meli E (1985), "The Earthquake: Causes and Effects in Mexico City," *Concrete International*, **8** (1986): 23–34.

Roy R (2009), "Inelastic Seismic Behavior of Multistoried Structures Highlighting the Effects of Asymmetry, Soil-flexibility, Degradation and Blast Loading," *Ph.D. Thesis*, Department of Civil Engineering, Bengal Engineering and Science University, Shibpur, Howrah, West Bengal, INDIA.

Rutenberg A (1992), "Nonlinear Response of Asymmetric Building Structures and Seismic Codes: a State of the Art Review," *European Earthquake Engineering*, **6**: 3–19.

Rutenberg A and Tso WK (2004), "Horizontally Irregular Structures: Some Recent Developments," *Proc. of International Workshop on Performance-based Seismic Design Concepts and Implementation*; Bled, Slovenia.

SEAOC, Vision 2000 (1995), "Performance Based Seismic Engineering of buildings," *Structural Engineers Association of California*, Sacramento, CA.

Sommer A and Bachmann H (2005) "Seismic Behavior of Asymmetric RC Wall Buildings: Principles and New Deformation-based Design Methods," *Earthquake Engineering and Structural Dynamics*, **34**(2):101–124.

Tso WK and Myslimaj B (2003), "A Yield Displacement Distribution-based Approach for Strength Assignment to Lateral Force-resisting Elements Having Strength Dependent Stiffness," *Earthquake Engineering and Structural Dynamics*, **32**(15): 2319–2351.

Tso WK and Zhu TJ (1992), "Design of Torsionally Unbalanced Structural Systems Based on Code Provisions I: Ductility Demand," *Earthquake Engineering and Structural Dynamics*, **21**(7): 609–627.

Zhu TJ and Tso WK (1992), "Design of Torsionally Unbalanced Structural Systems Based on Code Provisions II: Strength Distribution," *Earthquake Engineering and Structural Dynamics*, **21**(7): 629–644.

Appendix A: fundamental derivations

A1: Yield displacement eccentricity (CΔ^CM) and stiffness eccentricity (CR^CM)

Part-I: Yield displacement eccentricity (CΔ^CM)

Δ_{iy} **:** Yield displacement of structural element oriented along y-direction

$$\propto \frac{1}{l_{w_{iy}}} = \frac{c}{l_{w_{iy}}} \tag{A1.1}$$

where l_{wiy} = Length of the ith element and c = Constant.

Taking first moment of yield displacements of all elements about element line 1 (refer to Fig. 2(c)), results in,

$$\frac{c}{l_{w_{2y}}}\eta_{1\wedge 2x} + \frac{c}{l_{w_{3y}}}(\eta_{1\wedge 2x}+\eta_{2\wedge 3x}) + \ldots + \frac{c}{l_{w_{jy}}}(\eta_{1\wedge 2x}+\eta_{2\wedge 3x}+\ldots+\eta_{(j-1)\wedge jx}) + \ldots$$
$$+\frac{c}{l_{w_{ny}}}(\eta_{1\wedge 2x}+\eta_{2\wedge 3x}+\ldots+\eta_{(j-1)\wedge jx}+\ldots+\eta_{(n-1)\wedge n_x}) =$$
$$\left\{\sum_{j=2}^{n_y}\frac{1}{l_{w_{jy}}}\times\left(\sum_{j=2}^{j}\eta_{(j-1)\wedge j_x}\right)\right\} \tag{A1.2}$$

Thus, dividing Eq. (A1.2) by sum of the yield displacement of all elements, the distance of yield displacement center (CΔ) w.r.t. element line 1 may be expressed as

$$\left[\frac{1}{\sum_{i=1}^{n_y}\frac{1}{l_{w_{iy}}}}\left\{\sum_{j=2}^{n_y}\frac{1}{l_{w_{jy}}}\times\left(\sum_{j=2}^{j}\eta_{(j-1)\wedge j_x}\right)\right\}\right] \tag{A1.3}$$

Hence, the distance between the yield displacement center (CΔ) w.r.t. CM, i.e., yield displacement eccentricity ($C\Delta{\wedge}CM|_x$) along the x-direction may be expressed as

$$C\Delta{\wedge}CM|_x = \left[\frac{1}{\sum_{i=1}^{n_y}\frac{1}{l_{w_{iy}}}}\left\{\sum_{j=2}^{n_y}\frac{1}{l_{w_{jy}}}\times\left(\sum_{j=2}^{j}\eta_{(j-1)\wedge j_x}\right)\right\}\right] - \gamma_x D_x \tag{A1.4}$$

where γ_x defines the position of the center of mass normalized to D_x along the x-axis (Refer to Fig. 2c)

Part-II: Stiffness eccentricity (CR^CM)

K_{iy} **:** Stiffness of the structural element along the y-direction $= \frac{V_{niy}}{\Delta_{iy}} = \frac{\kappa_{iy}V_{ny}}{\frac{c}{l_{wiy}}} = \frac{V_{ny}}{c}\left(\kappa_{iy}l_{wiy}\right)$ (A1.5)

where V_{niy} = Nominal strength of ith element is oriented along the y-direction;

V_{ny} = Nominal strength of the system in the y-direction;

κ_{iy} = Relative strength distribution factor (ratio of strength of ith element to system strength in the y-direction)

Taking the first moment of stiffness of all elements about element line 1 (refer to Fig. 2(c)), results in

$$\frac{V_{ny}}{c}[\kappa_{2y}l_{w_{2y}}\eta_{1\wedge 2x} + \kappa_{3y}l_{w_{3y}}(\eta_{1\wedge 2x}+\eta_{2\wedge 3x}) + \ldots +$$
$$\kappa_{jy}l_{w_{jy}}(\eta_{1\wedge 2x}+\eta_{2\wedge 3x}+\ldots+\eta_{(j-1)\wedge jx}) + \ldots +$$
$$\kappa_{ny}l_{w_{ny}}(\eta_{1\wedge 2x}+\eta_{2\wedge 3x}+\ldots+\eta_{(j-1)\wedge jx}+\ldots+\eta_{(n-1)\wedge n_x})] =$$
$$\frac{V_{ny}}{c}\left\{\sum_{j=2}^{n_y}\kappa_{jy}l_{w_{jy}}\times\left(\sum_{j=2}^{j}\eta_{(j-1)\wedge j_x}\right)\right\} \quad \ldots\ldots\text{(A1.6)}$$

Thus, dividing Eq. (A1.6) by the sum of the stiffness of all elements, the distance of the center of resistance (CR) w.r.t. element line 1 may be expressed as

$$\left[\frac{1}{\sum_{i=1}^{n_y}\kappa_{iy}l_{w_{iy}}}\left\{\sum_{j=2}^{n_y}\kappa_{jy}l_{w_{jy}}\times\left(\sum_{j=2}^{j}\eta_{(j-1)\wedge j_x}\right)\right\}\right] \quad \ldots\text{(A1.7)}$$

Hence, the distance between the center of resistance (CR) w.r.t. CM, i.e., stiffness eccentricity ($CR{\wedge}CM|_x$) along the x-direction may be expressed as

$$CR{\wedge}CM|_x = \left[\frac{1}{\sum_{i=1}^{n_y}\kappa_{iy}l_{w_{iy}}}\left\{\sum_{j=2}^{n_y}\kappa_{jy}l_{w_{jy}}\times\left(\sum_{j=2}^{j}\eta_{(j-1)\wedge j_x}\right)\right\}\right] - \gamma_x D_x \tag{A1.8}$$

R.H. S. of Eqs. (A.1.4) and (A.1.8), for mathematical convenience, may be combined as

$$\left[\frac{1}{\sum_{i=1}^{n_y}\frac{\kappa_{iy}}{l_{wi_y}^{\ p}}}\left\{\sum_{j=2}^{n_y}\frac{\kappa_{jy}}{l_{wj_y}^{\ p}}\times\left(\sum_{j=2}^{j}\eta_{(j-1)\wedge j_x}\right)\right\}\right]-\gamma_x D_x \quad (A1.9)$$

where p = A mathematical exponent

For C$\Delta\wedge$CM $p = 1$ and $\kappa_{iy} = 1$;

For CR$\wedge$CM, $p = -1$ and κ_{iy} = ratio of strength of the ith element to the system strength

A2: Fundamental uncoupled lateral and torsional period

The fundamental uncoupled lateral period (T_l) may be estimated as under:

$$T_l = 2\pi\sqrt{\frac{M}{K}} \quad (A2.1)$$

where M = Mass lumped at story; K = Total lateral story stiffness = $\sum_{i=1}^{n_x}\frac{V_{nix}}{\Delta_{ix}}$ or $\sum_{i=1}^{n_y}\frac{V_{niy}}{\Delta_{iy}}$

V_{nix}, V_{njy} = Nominal strength of elements in the x and y directions, respectively;

Δ_{ix}, Δ_{jy} = Yield displacement of structural elements in the x and y directions, respectively, and may be estimated using the procedure outlined by Paulay (2001b) and Aschheim (2002);

n_x, n_y = Number of elements in the x and y directions;

Analogously, the fundamental uncoupled torsional period (T_θ) may be estimated as follows:

$$T_\theta = 2\pi\sqrt{\frac{I_M}{K_\theta}} \quad (A2.2)$$

where I_M = Mass moment of inertia about the reference center;

K_θ=Total torsional story stiffness= $\sum_{j=1}^{n_y}x_j^{\ 2}\frac{V_{niy}}{\Delta_{iy}}+\sum_{i=1}^{n_x}y_i^{\ 2}\frac{V_{nix}}{\Delta_{ix}}$

From Eqs. (AI2) ÷ (AI1), the ratio of uncoupled torsional-to-lateral period, τ may be estimated as follows:

$$\tau = \frac{T_\theta}{T_l} = \left[\frac{I_m}{M}\times\frac{K}{K_\theta}\right]^{\frac{1}{2}} = \left[\frac{Mr_g^{\ 2}}{M}\times\frac{K}{K_\theta}\right]^{\frac{1}{2}} = r_g\times\left[\frac{K}{K_\theta}\right]^{\frac{1}{2}} \quad \text{.......(A2.3)}$$

where x_j,y_i = distance of the elements from the reference center; r_g = Radius of gyration

APPENDIX B: Notations

Following symbols are used:

CV: center of strength of the system

CM: center of mass of the system

CR: center of resistance of the system

CΔ: yield displacement center

C$\Delta\wedge$CM$|_x$: distance between yield displacement center and center of mass in x direction

COV: co-efficient of variation

D_x, D_y: plan dimension of deck in x and y direction (taken here as equal to D)

e_v: distance between center of strength and center of mass

e_{rx} or e_{ry}: distance of CR from CM along x axis or y axis

e_{rr}: shortest distance between center of mass and center of stiffness

$e_{r\theta}$:angle of the joining CM and CR with x-axis

FD: earthquake having forward directivity

I: importance factor

I_M : mass moment of inertia about reference center

K: lateral stiffness of system

K_θ: torsional stiffness of system

l_{wi_y}: length of i^{th} wall oriented along y axis

LD: long duration earthquake

M: mass lumped at story

N: number of story

n_x, n_y: number of elements oriented in x and y direction

NHEDD: normalized hysteretic energy ductility demand

p: a mathematical exponent

PGA: peak ground acceleration

R: Response reduction factor, i.e., ratio of elastic strength demand to strength allocated to element

r_g: radius of gyration defining mass distribution

SD: short duration earthquake

T_l: lateral natural period of the system

T_θ: fundamental uncoupled torsional period

U_X^*: Deformation of element oriented in x-direction

U_Y^*: Deformation of element oriented in y-direction

$U(i)$: Displacement in ith degree of freedom

V_{nix}, V_{njy}: nominal strength of element in x and y direction

$\eta_{(j-1)\wedge j_x}$: distance between (j-1)th and jth element along x axis

γ_x: ratio of center of mass to plan dimension of deck along x axis

τ: fundamental uncoupled torsional-to-lateral period

κ_{iy}: ratio of ith element strength to strength of system in y direction

σ: standard deviation

μ_H: normalized hysteretic energy ductility demand

μ_{H0}: normalized hysteretic energy ductility demand for symmetric system

Δ_{iy} : yield displacement of element oriented along y direction